



The influence of Alkaline Granite addition on Ceramic Body Sintering

M. S. El-Maghraby¹, N. I. Abd El Ghaffar^{2*} and A. I. M. Ismail²



CrossMark

¹Ceramics, Refractories and Building Materials Department, National Research Centre, Dokki, Cairo, Egypt

²Geological Sciences Department, National Research Centre, Dokki, Cairo, Egypt

Abstract

Alkaline- granite was added on the ceramic bodies sintering at different temperatures from 1140°C to 1200°C. Four batches (50/50, 60/40, 70/30, 75/25) of granite to clay ratio were designed to investigate the effect of the granite/clay ratio on the phase composition and densification parameters.

Mineralogical and chemical composition of the starting raw materials was evaluated using XRD and XRF, phase composition, densification parameters, and microstructure of the fired batches were studied. The densification parameters decrease as increasing granite ratio and decreasing of clay. For the effect of the temperature, the bulk density, porosity, and water absorption decrease with increasing of the firing temperature, in batch no 1 and 2. Batch no 3, bulk density and linear shrinkage decrease, while apparent porosity and water absorption increase. Batch no 4. Bulk density and linear shrinkage decrease, apparent porosity and water absorption slightly increase till 1180°C and decrease at 1200°C. XRD and SEM with EDAX confirm that quartz and mullite are only two phases were detected.

Feldspar was totally replaced by alkaline granite in the formation of vitrified ceramic tile masses. Alkaline granite is better sintering behaviour it reduces the verification temperature and decreases the water absorption from 1140 to 1200°C. In the production of ceramic tiles, whitener of the fired product is not a required parameter; the substitution of feldspar for alkaline granite can be more beneficial due to the relatively higher cost of feldspars.

Keywords: Granite; Sintering; Clay; Ceramic Densification Parameters; Firing Temperature

1. Introduction

The ceramic tiles industries are the major consumer of the feldspar that act as fluxes and are composed mainly of potash feldspar and sodic feldspar. Due to the depletion of natural resources of feldspar, the recycling of granite wastes and weathered granites has attracted attention in the last few years in the ceramic industry as porcelain materials, tiles bodies, and all clay-based ceramic material (1-6).

Feldspars are the main constituents of albitites, granites, and acidic varieties as well as feldspathoidal sand (7–11). They are responsible for the formation

of the glassy phase, which leads to the sintering of the ceramic body. K feldspar decreases the thermal shrinkage whereas sodium feldspar decreases the thermal expansion and fuses at lower temperatures compared with other fluxes. Other raw materials, such as pegmatite, basalt, nepheline syenite, phonolites, and perlites are widely used in ceramic industries as fluxing substances, (12–15).

Granites are widely distributed in the continental crust of the earth and are considered an important rock group that covers wide areas of the Arabian-Nubian Shield in Egypt. It constitutes about 40 % of the total basement complex of Egypt (16-17). Many

*Corresponding author e-mail: nahla169@yahoo.com (N. I. Abd El Ghaffar)

Received date 14 September 2022; revised date 15 December 2022; accepted date 21 December 2022

DOI: 10.21608/EJCHEM.2022.162951.6982

©2023 National Information and Documentation Center (NIDOC)

authors used the granite in different sources as powder waste from sawing processes of ornamental stones, fresh and weathered rocks in the ceramic tile industries and concluded that about 15–40 % of granite can be used for the production of red stoneware tiles using rapid-firing cycles and fired at 1200–1300°C [18-19]. Granite is considered a flux material due to its large amount of alkali oxides as K₂O and Na₂O. The main sources of these oxides are feldspars, alkali pyroxenes, and amphiboles which are common constituents of alkaline granites. It was noted that the granite components allowed better sintering properties as compared with the feldspar, by decreasing the sintering temperature. The incorporation of granite waste into ceramic products also represents a good way using of this waste in a useful industry (20).

The depletion of the main flux feldspathoidal sources in the World (Pegmatites and albitites), against the increase of the global demand, is leading the ceramic researchers to find other suitable alternatives. Among the potential substitutes are alkaline acidic igneous rocks, including alkaline granite (riebeckite bearing granites). One of the most promising areas for alkaline granite occurrences is Southern Sinai.

Granitoids represented about 70% of the basement complex of Sinai basement rocks (21). The A-type granites (Riebeckite bearing granites and alkali feldspar granites) constitute vast areas in Sinai comparing any other region of the Arabian-Nubian Shield, accounting for 20% of all granitic rocks alkaline, granites, syenitic rocks, and their volcanic equivalents. The investigated area is situated in southern Sinai and easily accessible through Dahab-Sharm El Sheikh asphaltic road.

2. Geological setting

The investigated area lies between latitudes 28° 03' - 28 ° 14' N and longitudes 34 ° 05' E- 34° 16' E Fig. 1. The basement rocks located in the studied area are sequentially arranged as 1- Metavolcanics, 2- Older granite, 3- Younger granite (phase 2& 3), and 3- Riebeckite granite (22). Field observations indicate that riebeckite-bearing granites are the youngest rock unit that forms high elevated mountains concerning the adjacent G-2 granites.

These rocks intrude directly Younger granite phase II with sharp intrusive contact Fig. 2. Few xenoliths are recorded within riebeckite-bearing granites with

sharp contact. These rocks are fresh with gray color and consist mainly of alkali feldspars, quartz, plagioclase, and riebeckite.

The aim of the current work is to assess the effect of the weathered alkaline granite addition on the sintering behavior of the ceramic bodies as firing at different temperatures from 1140°C to 1200°C with an interval of 200°C. To perform that, four batches with different ratios of weathered granite and clay were designed and fired at different temperatures. Chemical and mineral composition of the starting materials was carried out, densification parameters and phase composition, as well as microstructure of the fired batches, was studied. Optimum additives of weathered granite and firing temperature were estimated

3.1. Materials

Egyptian clay and riebeckite bearing granite are the main raw materials used in the present work. Egyptian clay of El-Ogybab area, northeaster part of Aswan governorate in southern Egypt. The clay was obtained from Normatic Co. for building materials and refractories, Helwan, Cairo, Egypt. Sodium tripolyphosphate was bought from El-Gomhoryia Company. The riebeckite bearing granite aggregates were collected from Wadi Adawi area, which is situated in the eastern part of South Sinai about 22 Km from Dahab-Sharm El Sheikh asphaltic road, riebeckite bearing granite samples were collected as aggregates with different sizes (24, 25).

3.2 Methods

The alkaline granite samples were petrographically identified in thin sections using the Polarized Microscope. Clay materials and alkaline granite rock were mashed, ground, and sieved by 63 µm sieves by milling in wet situations (15 min in a planetary mill with porcelain jar and porcelain grinding media). The slip obtained (~70% solid load, 0.3% Na-tripolyphosphate) was oven-dried and disagglomerated before manual granulation. Powders were shaped into 30 × 30 × 5 mm tiles by hydraulic pressing (35 MPa) then dried in an oven (110 °C overnight) and fast fired in an electric furnace (temperature from 1140 °C to 1200 °C; 30 min. soaking time). Their chemical and mineralogical characteristics are carried out using XRD, XRF respectively. Scanning electron microscope (SEM) has been applied in the current work to detect the textural features and mineral identifications as well as mineral chemistry.

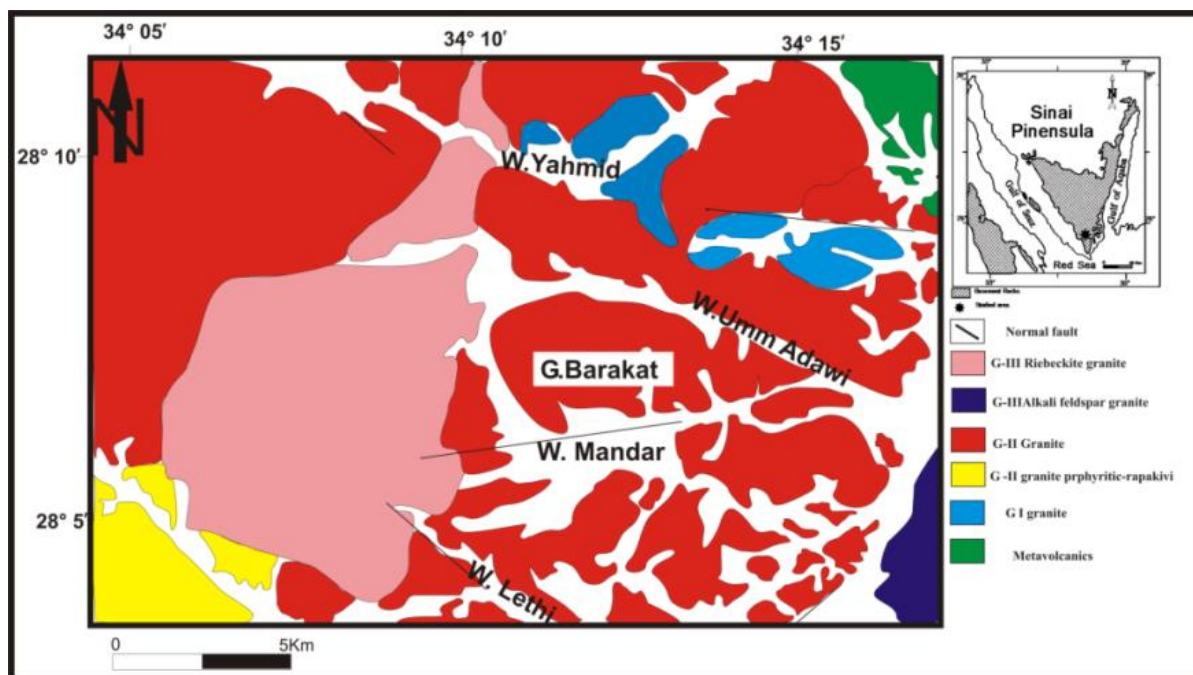


Fig. 1. Geological map of Wadi Mandar area after Abd El Ghaffar and Ramadan, 2018.

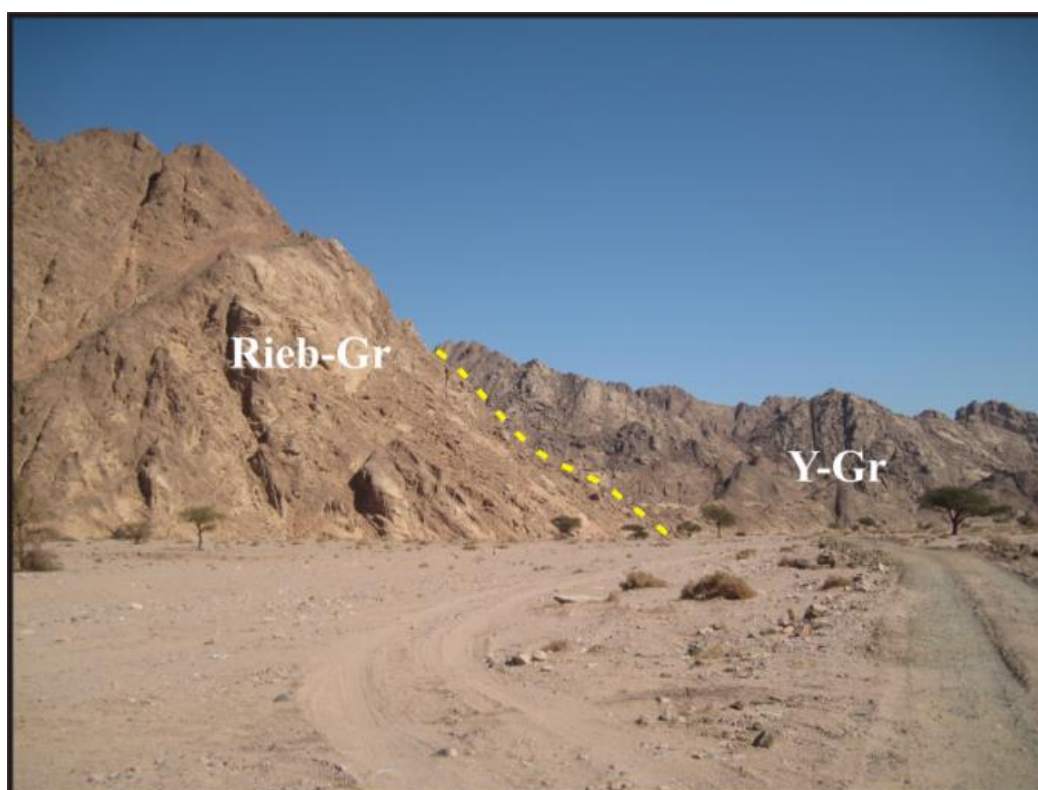


Fig.2. Displays sharp intrusive contact between Younger Granite(Y-Gr) and Riebeckite bearing granite(Rieb-Gr).

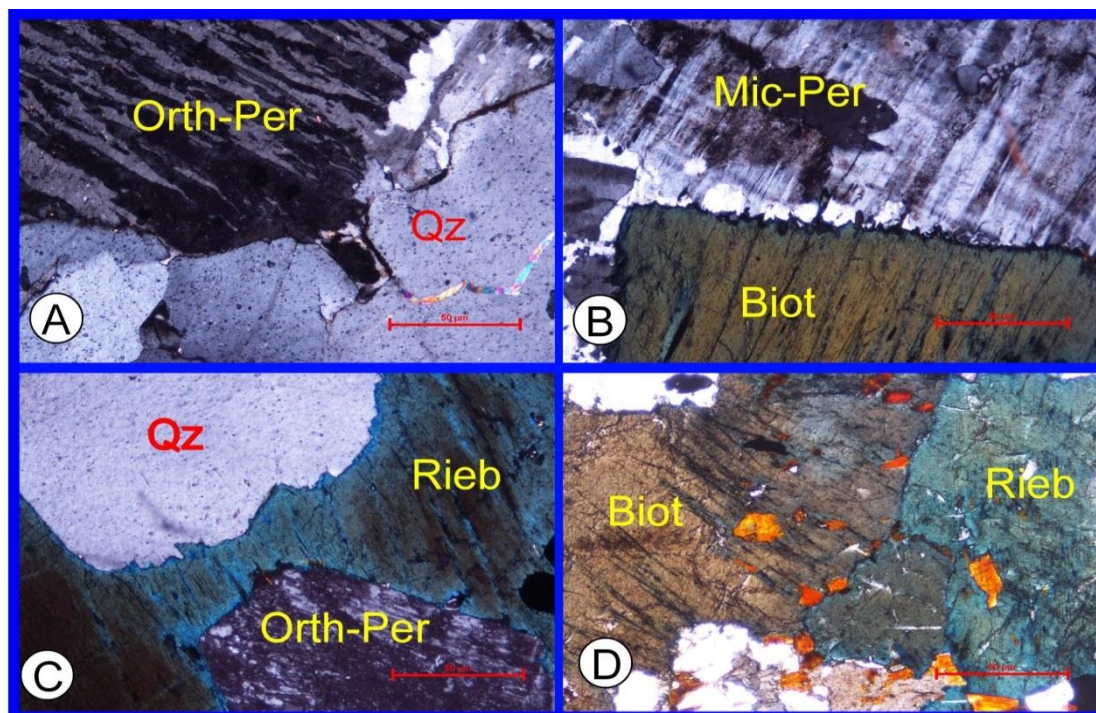


Fig.3.A. Association of orthoclase perthite (Orth-per) and quartz (Qz), **B.** Association of microcline perthite and biotite (biot), **C.** Riebeckite (Rieb) crystal invaded by orthoclase perthite (Orth-per) crystal. **D.** Scattered allanite crystals associated with biotite (biot) and Riebeckite (Rieb).

The properties of the studied samples were technologically evaluated in dry conditions and after firing at 1200 °C; after 30 minutes. Bulk density and linear shrinkage and were estimated for all samples; while, apparent porosity and water absorption were estimated for fired samples. Water absorption, linear shrinkage, bulk density and porosity are plotted versus the firing temperatures for drawing the sintering curves. The obtained phases, microstructures, and mineral-chemistry of some fired batches, were determined using XRD and SEM as well as EDAX, respectively.

In terms of apparent porosity and bulk density the densification properties were also estimated using water displacement methods (26, 27).

4. Results and Discussion

Riebeckite bearing granites (Alkaline granites) are massive and medium-grained. These rocks show hypidiomorphic to panidiomorphic granular textures. Microscopically, these rocks are composed mainly of alkali feldspars 58.8 %, quartz 33.6%, plagioclase feldspar 16.1 %, riebeckite 2.7%, and biotite 0.7%.

Accessory minerals are represented by zircon, apatite, allanite, and iron oxides attaining 0.08 %.

Alkali feldspars exist as orthoclase microperthite and microcline microperthite Fig. 3 A&B. The former is represented by subhedral crystals ranging from up to 5.3x 3.1mm in dimensions. It comprises patches, veins, veinlets, and strings of perthitic intergrowth. The crystals are variably altered to muscovite and kaolinite, while the latter exists as anhedral to subhedral crystals reaching up to 3.1x 5.2 mm in dimensions.

Quartz occurs as subhedral to anhedral irregular crystals (0.7x1.66 mm) partly replacing and embaying the alkali feldspars forming graphic and granophyric textures. In some cases, the crystals are interstitially filling spaces and poikilitically enclosed in alkali feldspars.

Riebeckite (Fig. 3 C.) exists as subhedral to anhedral cleavable crystals of dark blue color. Riebeckite forms long prismatic crystals up to 4.3 X 3.2 mm in dimensions. Some crystals attain fibrous and asbestiform shapes. It is generally altered to chlorite

and opaques, especially along cleavage planes and crystal peripheries.

Biotite (Fig.3 B&D) presented as anhedral flakes altered to chlorite and iron oxides. Plagioclase presents as subhedral crystals showing albite type of twinning. They have an albite composition of An5-8 reaching up to 3.2 to 2.1 mm in diameters.

Allanite (Fig. 3D) and apatite occur as scattered small crystals sometimes are of close association with mafic phases.

The major oxides content of the start raw materials (chemical composition) were obtained using the XRF technique as previously illustrated in Table 1. The major oxides of the granite deposits are SiO₂, Al₂O₃, Na₂O, and K₂O as 74.92, 12.81, 4.39, and 4.18%, respectively. Lesser amounts of Fe₂O₃ are detected (1.97%) with minor amounts of CaO and MgO being 0.35 and 0.32%, respectively. Traces of TiO₂ and SO₃ were also observed while L.O.I of the sample has a value of 0.58%. The chemical composition of the clay used in this work indicates that silica, alumina, iron oxide, and titania are the major components in the following percentage 52.97, 29.07, 3.92, and 1.48%. Loss on ignition is 10.62%.

XRD of the starting raw materials used in current show that the main mineralogical composition of granite is quartz, microcline, and albite, which match the chemical composition carried out by XRF. The mineral composition of the clay is halloysite and kaolinite (clay minerals) and quartz (non-clay mineral), Fig. 4.

Four batches were designed to assess the effect of the granite/clay ratio on the densification parameters as well as the microstructure of these batches at different firing temperatures, such as 50/50, 60/40, 70/30, 75/25 of granite to clay ratio. The main

compositions of the four batches are SiO₂, Al₂O₃, Na₂O, K₂O, and Fe₂O₃. Silica ranges from 63.95% in batch no. 1 and increases to 69.43% in batch no. 4 as granite increase, while Al₂O₃% decreases from 20.94 in batch 1 to 16.88 in batch no. 4 by decreasing the clay content of the batches. Sodium and potassium oxides percentages also show higher values as the increase of granite content as a fluxing agent. Total iron has higher values in batch no. 1 as 2.95% compared with batch no. 4 (2.46%) by reducing the clay content rich in iron.

The chemical composition (Tables. 2,3,4&5) refers that the batches with high content of granite rich in silica as well as sodium and potassium oxides, while batches containing high content of clay are rich in alumina and iron oxides.

In terms of bulk density and shrinkage, Some densification parameters for the green batches illustrated that the density decreased from 2.12g/cm³ in batch 1 to 1.90 cm³ in batch no. 4as increase in clay content, while shrinkage decrease by increasing granite content from batch no 1 +0.75% to +0.46% in batch no. 4 as illustrated in table 6.

Two varieties control the physical properties of these batches, the batch composition, which refers to the granite/clay ratio, and the firing temperature. So, we will study their properties by establishing one variety and changing the other, Fig. 5.

At 1140°C, the bulk density for the four batches shows a slight change in values within 2.29-2.32g/cm³, while the apparent porosity shows a highly decreasing by the granite ratio from 7.37 in batch no. 1 to 0.01% in batch no. 4. Water absorption also decreased, while linear shrinkage slightly changed.

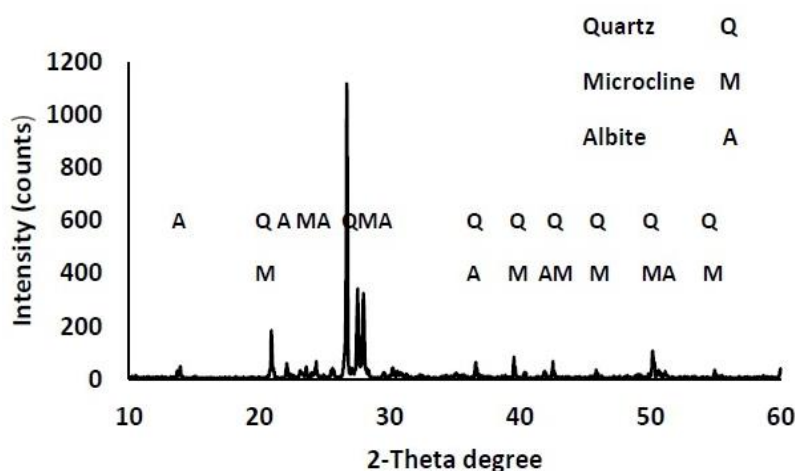


Fig. 4 XRD pattern of the alkaline granite.

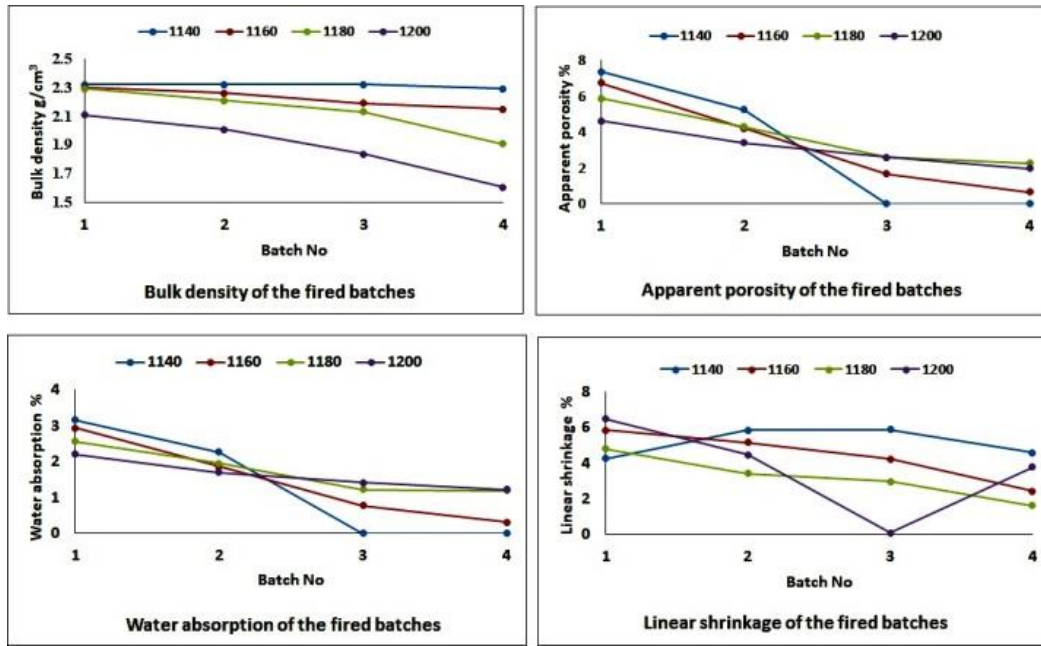


Fig. 5. Water absorption and shrinkage of the fired batches.

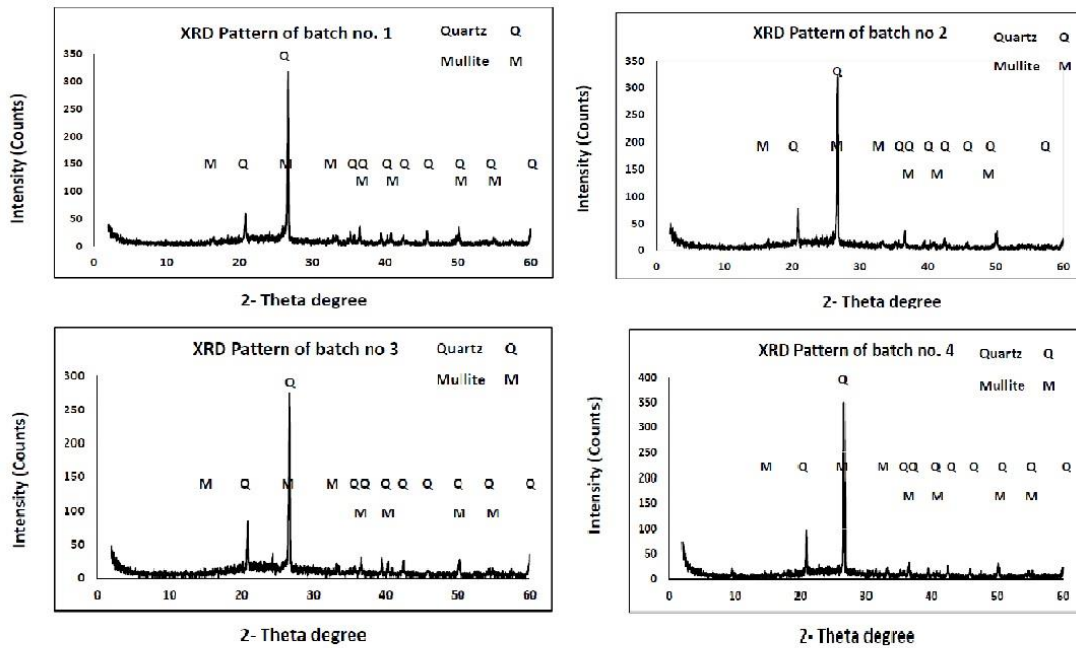


Fig. 6. XRD of the fired batches.

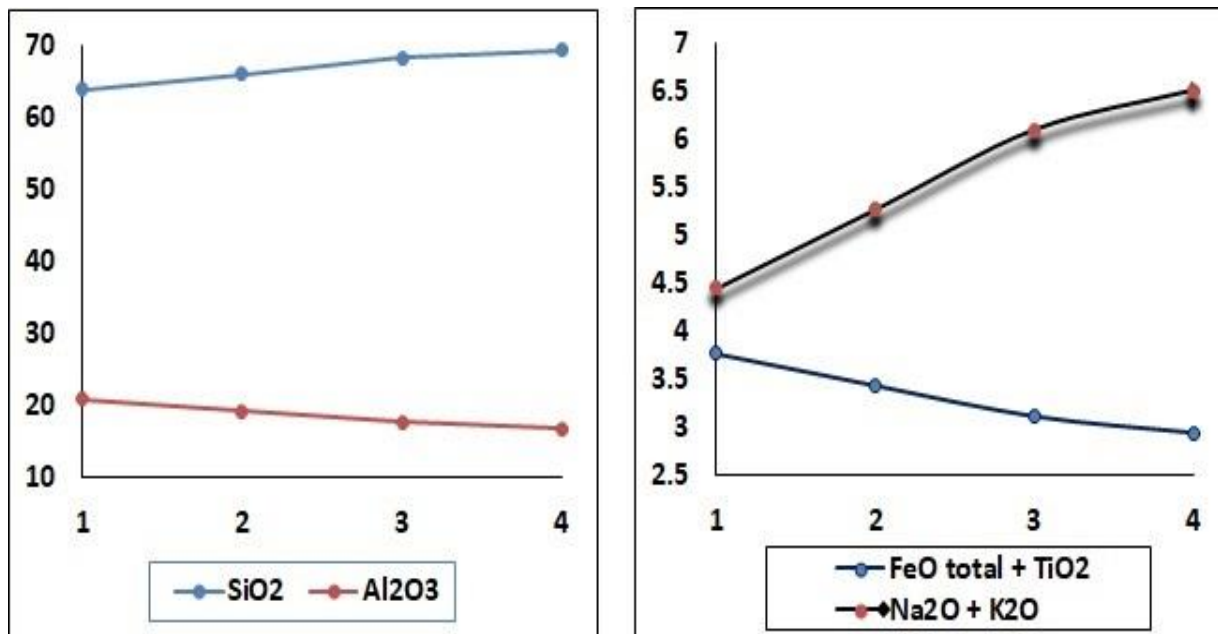


Fig. 7. Content of silica, alumina, alkalis and iron oxides in the four batches.

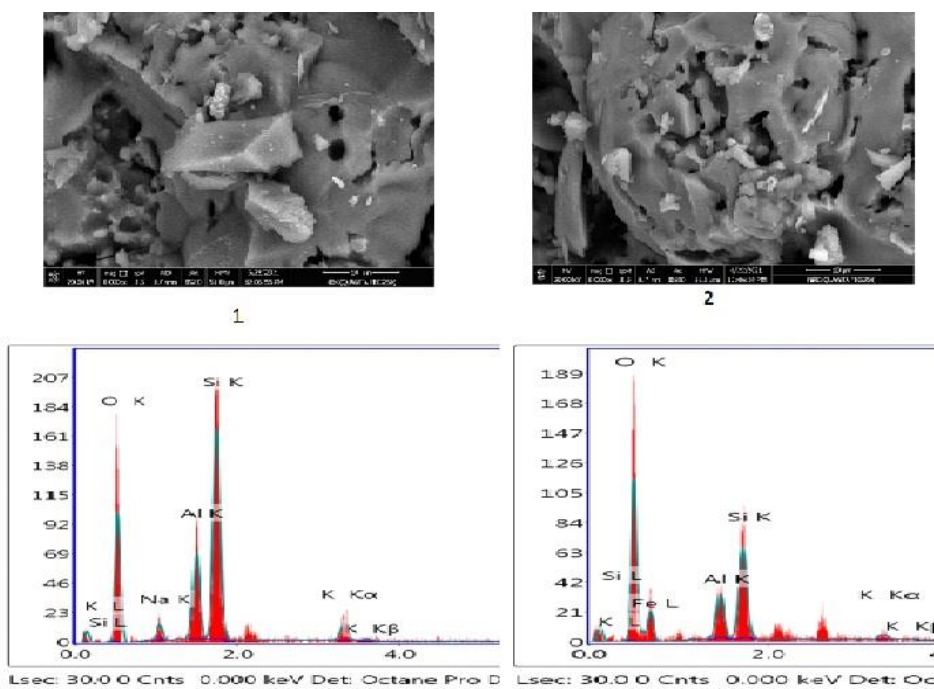


Fig. 8. SEM and EDAX of the batch no 1 fired at 1140 °C.

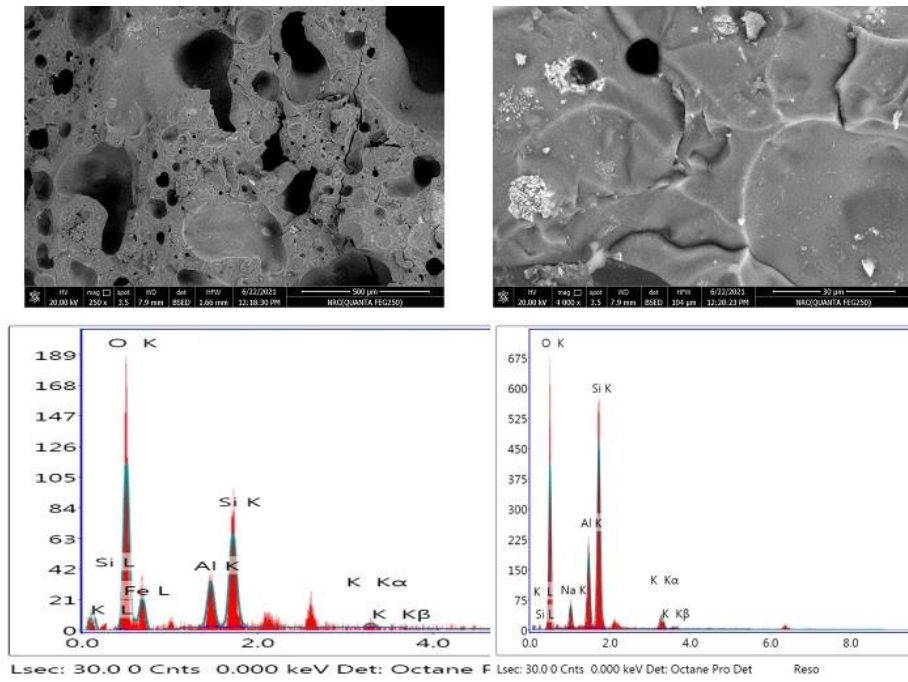


Fig. 9. SEM and EDAX of the batch no 1 fired at 1200 °C.

Table 1: Chemical composition of the used raw materials

Oxides %	Granite	Clay
SiO ₂	74.92	52.97
Al ₂ O ₃	12.81	29.07
TiO ₂	0.16	1.48
Fe ₂ O ₃	1.97	3.92
CaO	0.35	0.5
MgO	0.32	0.2
Na ₂ O	4.39	0.06
K ₂ O	4.18	0.28
SO ₃	0.01	0.76
LOI	0.58	10.62
Total	99.84	99.86

Table 2: Chemical composition of the design batch no. 1

Oxides %	50 granite	50 clay	Total
SiO ₂	37.46	26.485	63.95
Al ₂ O ₃	6.405	14.535	20.94
TiO ₂	0.08	0.74	0.82
Fe ₂ O ₃	0.985	1.96	2.95
CaO	0.175	0.25	0.43
MgO	0.16	0.1	0.26
Na ₂ O	2.195	0.03	2.23
K ₂ O	2.09	0.14	2.23
SO ₃	0.005	0.38	0.39
LOI	0.29	5.31	5.60
Total	49.92	49.93	99.85

Table 3: Chemical composition of the design batch no. 2

Oxides %	60 granite	40 clay	Total
SiO ₂	44.952	21.188	66.14
Al ₂ O ₃	7.686	11.628	19.31
TiO ₂	0.096	0.592	0.69
Fe ₂ O ₃	1.182	1.568	2.75
CaO	0.21	0.2	0.41
MgO	0.192	0.08	0.27
Na ₂ O	2.634	0.024	2.66
K ₂ O	2.508	0.112	2.62
SO ₃	0.006	0.304	0.31
LOI	0.348	4.248	4.60
Total	59.904	39.944	99.76

Table 4: Chemical composition of the design batch no. 3

Oxides %	70 granite	30 clay	Total
SiO ₂	52.444	15.891	68.34
Al ₂ O ₃	8.967	8.721	17.69
TiO ₂	0.112	0.444	0.56
Fe ₂ O ₃	1.379	1.176	2.56
CaO	0.245	0.15	0.40
MgO	0.224	0.06	0.28
Na ₂ O	3.073	0.018	3.10
K ₂ O	2.926	0.084	3.01
SO ₃	0.007	0.228	0.24
LOI	0.406	3.186	3.59
Total	69.888	29.958	99.77

Table 5: Chemical composition of the design batch no. 4

Oxides %	75 granite	25 clay	Total
SiO ₂	56.19	13.2425	69.43
Al ₂ O ₃	9.6075	7.2675	16.88
TiO ₂	0.12	0.37	0.49
Fe ₂ O ₃	1.4775	0.98	2.46
CaO	0.2625	0.125	0.39
MgO	0.24	0.05	0.29
Na ₂ O	3.2925	0.015	3.31
K ₂ O	3.135	0.07	3.21
SO ₃	0.0075	0.19	0.20
LOI	0.435	2.655	3.09
Total	74.88	24.965	99.85

Table.6 :Density and linear shrinkage of the green batches

Batch no.	1	2	3	4
Density	2.12	2.05	1.97	2.07
Shrinkage	+0.75	+0.60	+0.54	+0.46

At 1160°C, bulk density and linear shrinkage are slightly decreased by increasing the granite content from 2.30 to 2.15g/cm³ and 5.86 to 2.45% for the bulk density and linear shrinkage, respectively. Apparent porosity and water absorption show highly decrease from 6.77 to 0.67% and 2.94 to 0.31%, respectively.

At 1180°C, all the parameters show lower values by increasing the granite content in this range, density (2.29-1.91g/cm³), porosity (5.88-2.29%), water absorption (2.57-1.20%), and linear shrinkage (4.81-1.64%).

At 1200°C, bulk density, apparent porosity and water absorption decrease by increasing the granite content from 2.11 to 1.61g/cm³ for bulk density, 4.64 to 1.98% for apparent porosity, and 2.21 to 1.23% for water absorption. Linear shrinkage decreased in regular order from batch no. 1 to 3 (6.49-0.1%) and increase to 3.80% in batch no 4. It is noted that change in porosity is not accompanied by a notable change in density.

In general, we can conclude that by increasing the granite ratio and decreasing the clay the densification parameters decrease (Table.7).

For the effect of the temperature on each batch, it is noticed that the bulk density, porosity, and water absorption decrease with increasing of the firing temperature, while water absorption irregular decreases from 4-6%, in batch no 1.

For batch no 2 by increasing the firing temperature, the bulk density, porosity, and water absorption decrease, while linear shrinkage decrease to 1180°C and begin to increase up to 1200°C. In batch no 3, with the increase of firing temperature, bulk density, and linear shrinkage decrease, while apparent porosity and water absorption increase. Batch no 4. Bulk density decrease, apparent porosity slightly increases till 1180°C and decrease at 1200°C. Water absorption slightly increases, while linear shrinkage decreases till 1180°C and increases at 1200°C.

XRD studies for the phase composition of the fired batches at 1160°C confirms that only two phases were detected in the four batches. Quartz and mullite with high crystallinity and intensity were recorded.

From the results of XRF and XRD, we can conclude that mullite and quartz are only two phases formed at all temperature and batch compositions. Batch no. 1 contains the highest value of alumina so

it is expected to be rich in mullite than the others and the liquid phase formed contains high iron content and fewer alkalis so it is more viscous, Fig. 6. By increasing the granite content alkalis increase and iron content decrease so liquid phase viscosity decrease as well as mullite and quartz content decrease. It is expected that mullite content from batch 1 to 4 and the liquid phase increase at expense of quartz and mullite. So, it may attribute to reduction of density and porosity with high temperature and granite content and forming low density rich in alkalis.

Tables 8&9 and figure 7 show the content of silica, alumina, alkalis, and iron oxides in the four batches. It is clear that silica and (Na₂O + K₂O), while alumina and (total iron + TiO₂), decrease. So, batch no 1 is rich in alumina, total iron, and titania and lesser in alkalis and silica.

Microstructure studies of batch no 1 and 4 fired at 1140°C was performed by scanning electron microscope and EDAX as shown in figure 8&9.

Figures 8 &9 depict the microstructures of batch no. 1 fired at 1140 °C and 1200°C as recognized by scanning electron microscope. Both fired temperature batch shows that the microstructure is composed of distorted mullite set in a matrix of siliceous glassy phase. Relics of primary mullite embedded in a glassy groundmass composed of silicates of sodium, potassium, aluminum, iron, and titanium as illustrated by EDAX. Quartz did not appear as crystals in the microstructure but was recorded as silicate glassy phase. High alkalis contents lead to re-dissociation of the preformed crystals of mullite and quartz as well as increase the liquid phase content.

The microstructure of the fired batch at 1200°C, Figure 9, as revealed from scanning electron microscope and EDAX, shows that at high firing temperature the liquid phase increase till leaked leading to an increase in the porosity and decrease the density, as well as high pores and micro-fracture, are observed. Both batches show microstructure consisting of mullite set in a matrix of siliceous glassy phases. The phase composition of the batches was determined using the XRD technique. The X-ray patterns refer to the existence of both quartz and mullite as the main phases in the fired batches.

5. Conclusion:

Egyptian weathered alkaline granite and clays are the raw materials used in this study. XRD

studies show that the main mineral composition of granite is quartz, microcline, and albite, which match to the chemical composition carried out by XRF.

Microscopically, these rocks are composed mainly of alkali feldspars, quartz, plagioclase feldspar, riebeckite, and biotite.

The mineralogical composition of the clay is halloysite and kaolinite as clay mineral and quartz as a non-clay mineral.

Four batches were designed to investigate the effect of the granite/clay ratio and firing temperature on the densification parameters and phase composition as well as the microstructure. XRD study confirms that quartz and mullite are only two phases were detected in the fired batches.

It is noticed that, with increasing the firing temperature, the bulk density, apparent porosity, and water absorption decrease, in batch no 1 and 2. While in batch no 3, bulk density and linear shrinkage decrease, apparent porosity, and water absorption increase. Batch no 4. and linear shrinkage and bulk density decrease apparent porosity and water absorption slightly increase till 1180°C and decrease at 1200°C.

Microstructure studies of the fired batch at 1140 & 1200°C were performed by scanning electron microscope and EDAX confirmed that anhedral crystals of mullite within siliceous groundmass as illustrated by XRD. By increasing the firing temperature the liquid phase increase at the expense of the mullite and quartz phases.

It is concluded that feldspar was totally replaced by alkaline granite in the formation of vitrified ceramic tile bodies and alkaline granite is better sintering properties as reducing the vitrification temperature. It is concluded that alkaline granite is better sintering properties as reducing the vitrification temperature.

Acknowledgment

The support for this research was provided by the National Research Centre through project number 12010307 .

Conflict of Interest

The authors declare that they have no competing financial interests or personal relationships that could have appeared to influence this work.

References

- [1] Hernandez-Crespo M.S. and Rincon, J.Ma (2001). New porcelainized stoneware materials were obtained by recycling MSW incinerator fly ashes and granite sawing residues. *Ceram. Int.*, 27, 713-720.
- [2] Monteiro, S.N.,Pecanha, L.A. and Vieira, C.M.F., (2004). Reformulation of roofing tiles body with the addition of granite waste from sawing operations. *J. Eur. Ceram. Soc.*, 24, 2349-2356.
- [3] Ayangade, J.A. Olusola, K.O. Ikpo, I.J. and Ata, O. (2004). Effect of granite dust on the performance characteristics of kernelrazzo floor finish. *Building and Environ.* 39, 1207- 1212.
- [4] Menezes, R. R., Ferreira, H.S., Neves, G.A., Lira, H.L. and H.C. Ferreira, (2005). Use of granite sawing wastes in the production of ceramic bricks and tiles". *J. Eur. Ceram. Soc.*, 25, 1149-1158.
- [5] Segadaes, A. M. Carvalho, M.A.andAcchar, W., (2005).Using marble and granite rejects to enhance the processing of clay products". *Appl. Clay Sci.*, 30, 42-52.
- [6] P. Torres, H.R. Fernandes, S. Agathopoulos, D.U. Tulyaganov, and J.M.F Ferreira, "Incorporation of granite cutting sludge in industrial porcelain tile formulations". *J. Eur. Ceram. Soc.*, 24, 3177-3185 (2004).
- [7] ElMaghraby, M. S. Ismail A. I. M. &Shalaby, B. N. A.(2021). Utilization of some Egyptian Raw Materials in Ceramic Tiles, *Silicon* 13:985–992.
- [8] Kingery, W. D (1960).Introduction to ceramics, John Wiley and Sons, Inc., New York, P.N. 781.
- [9] Mostafa A.(1989). Ceramic floor tiles from Egyptian raw materials, M.Sc. Thesis, Faculty of Science, Zagazig University
- [10]Joshi, C. K. Malkan, V. G..Bhatt, J. V, (1993).Ceramic raw materials of India. Seminar on ceramic industry raw materials & essential inputs, Ahmedabad, 3–44.
- [11] Youssef, N. F. Shater, M. O. Abadir, M. F. and Ibrahim, O. A. (2002). Utilization of red mud in the manufacture of ceramic tiles. *KeyEng. Mater* 206-213:1775–1778.
- [12]Dinsdale. A(1986). Pottery Science Materials, Process, and Products. Ellis Horwood Ltd., West Sussex, U. K, ISBN 10:0470202769 ISBN 13: 9780470202760.
- [13]Kobayashi, Y. O., Ohira, Y. O Kato, E. (1992). Vitrification of Whiteware bodies in alumina-feldspar-kaolin system. *J Jpn Ceram Soc* 100(5):743–749.
- [14]Dondi, M., Guarini, G., Venturi, I. (2001). Assessing the fusibility of feldspathic fluxes for ceramic tiles by hot stage microscope. *Ind. Ceram* 21:67–73.
- [15]El- Fadaly, E. (2013). Characterization of Porcelain Stoneware Tiles Based on Solid Ceramic Wastes, *International Journal of Science and Research (IJSR)* ISSN, 2319–7064, P. 602–608. ISSN (Online): 2319–7064.

- [16] Naga, S. M. El-Nashar, E.R., El-Omla M. and Abd El-Shakour, Z.(2012). Porcelainized stoneware tiles based on Egyptian granite, *Interceram*, 61(5):286-290.
- [17]Leake, B. E. , Brown, G. C. Halliday, A. N. (1980). The origin of granite magmas: a discussion. *J. Geol. Soc. London*137, 93–97.
- [18]Ibrahim, D. M. . Sallam E.H and Naga, S.M. (1990). Effect of the degree of crystallinity of flux on tile bodies. *Tile & Brick* 6, 4223.
- [19]Vieira, C. M. F. andMonteiro, S. N. , (2000). Incorporation of Granite Waste into Vitrified Ceramic Tiles, State University of the North Fluminense Darcy Ribeiro-UENF, Advanced Materials Laboratory-LAMAV, Av. Alberto Lamago, 28013-602, Campos dos Goytacazes-RJ, Brazil.
- [20]El-Maghraby, H. F. El-Omla, M. M.,Bondioli, F ,Naga, S. M. Granite as flux in stoneware tile manufacturing *J. Eur. Ceram. Soc.* **31**, 2057–2063,(2011).
- [21]. Bentor. Y.K (1985).The crustal evolution of the Arabo-Nubian Massif with special reference to the Sinai Peninsula. *Precambrian Research* 28, 1–74.
- [22]Ahmed, M.A. (1985). Geological studies of some granitic rocks of WadiAdawi, Southeastern Sinai. Ph.D. Al Azhar Univ. Cairo. Egypt.
- [23]Abd El Ghaffar, N. I. and Ramadan, A. A. (2018). Geochemistry and origin of alkaline granites at Wadi Umm Adawi-Yahmid area, south Sinai- Egypt., *J. African Earth Sci.* 146 , 66-77.
- [24]Shalaby, B. N., El- Maghraby M. S & Ismail, A. I. , (2018). Technological properties of high alumina refractories with different phosphoric acid Contents, *Bulletin of the National Research Centre*, 42:24.
- [25]Ismail, A. I. M., Elmaghraby M. S. andAbd El Ghaffar, N. I. (2021).Effect of Granite Weathered Granules Additives as Aggregates in Cement Concrete, *Egypt. J. Chem.* Vol. 64, 3, 1553 – 1562,
- [26]Nishikawa, A. (1984). Technology of monolithic refractories. Plibrico Japan Company Ltd., shiba 5 chome, Minato-Ku, Tokyo (Japan) No 33–7.
- [27]Serry, M. A., Ahmed S.E. andElmaghray, M. S. (2007). Shaped MgO-Al₂O₃-SiO₂ refractory ceramics from recycled materials. *Advances in applied ceramics* 106, 149–154.